VORTEX-JET MECHANISM IN A CHANNEL WITH SPHERICAL DIMPLES FOR HEAT TRANSFER AUGMENTATION

Johann Turnow, Nikolai Kornev, Sergej Isaev, Egon Hassel

Department of Mechanical Engineering
Institute of Technical Thermodynamics
University of Rostock
Albert-Einstein-Str. 2,D-18059 Rostock, Germany
johann.turnow@uni-rostock.de

ABSTRACT

Vortex mechanism of heat transfer enhancement in a narrow channel with dimples has been investigated numerically using LES method. The flow separation results in a formation of vortex structures which significantly enhance heat transfer on dimpled surfaces conducted by a small increase of the pressure loss. The heat transfer To get a deep insight into flow physics LES is performed for single phase flow in a channel with a spherical dimple. The instantaneous vortex formation and separation are investigated inside the dimple area. Considered are Reynolds numbers (based on dimple print diameter) $Re_D = 20000$ and $Re_D = 40000$ and the depth to print diameter ratio of $\Delta = 0.26$. Frequency analysis of LES data revealed the presence of two dominating frequencies in unsteady flow oscillations. Direct analysis of the flow field revealed the presence of coherent vortex structure inclined to the mean flow. The structure changes its orientation in time causing the long period oscillations with opposite-of-phase motion. Three dimensional proper orthogonal decomposition (POD) analysis is carried out on LES pressure and velocity fields to identify spatio-temporal structures hidden in the random fluctuations. Tornado-like spatial POD structures have been determined inside dimples.

INTRODUCTION

Vortex enhancement of heat transfer caused by turbulators is currently used in modern heat exchangers. In case of using dimples as turbulators the hydrodynamic and thermodynamic properties of exchangers become optimal in comparison with other heat transfer enhancement methods like ribs and fins. Especially with respect to the pressure loss this innovative cooling method shows major advantage as compared with existing conventional methods. Basically the physics of the flow inside the dimple is complicated and it is still not completely understood. Main attention of papers published in the literature has been paid to the heat and mass transfer effects averaged in time whereas the unsteady processes and their role in the heat transfer enhancement have not been thoroughly investigated. The structure of vortices created within dimples remains not quite clear especially when the flow is highly unsteady at large depth to diameter ratio of the dimple. Since the form of the vortex has a strong impact on the heat transfer the deep understanding of physics inside of the dimple is important for the further improvement heat exchanger efficiency.

The first investigations of unsteady effects were performed by Gromov et al. (1986) who presented the picture of vortex formation in a single dimple. More detailed investigation was performed by Terekhov et al. (1997) who documented periodical outbursts of vortices from downstream rim using hydrogen bubbles. Transverse oscillations of the outbursts with low ($\omega < 1Hz$) and high frequency ($\omega > 1Hz$) were observed at the Reynolds numbers up to $Re_D = 40000$. Analysis of instantaneous pictures of the flow revealed a consequent process of generation of regular vortices in the recirculation zone, their shedding downstream resulted in the formation of staggered rows of vortices. Unfortunately, these first valuable observations have never been quantified properly and analyzed in the further investigations using modern nonintrusive measurement techniques and advanced numerical technologies like LES and DNS. The most detailed experimental study of unsteady flow characteristics on dimpled packages has been performed by (Mahmood et al., 2000; Ligrani et al., 2001; Won et al., 2005). Flow visualisation by smoke patterns revealed a primary vortex pair generating periodically in the center of the hole. Additionally to the primary vortex pair two secondary vortices arise at the spanwise edges of each dimple. Furthermore for dimples with a depth to diameter ratio of $t/D \geq 0.22$ a significant augmentation of heat transfer is documented, when dynamic vortex structures with transversal oscillations occur around dimple area. In fact, at present there exists no generally accepted point of view regarding the vortex formation both in a single dimple and on dimple packages. Different scenarios are published in the literature.

The vortex flow within a dimple is definitely highly unsteady and a single steady coherent vortex structure doesn't exist. The flow reveals the presence of two dominant modes whereas one of them changes the position at low frequency. The reason for such a flow behaviour is still not clear. Since the form of the vortex has a strong impact on the heat transfer the deep understanding of physics inside the dimple is important for the further improvement of dimple exchanger efficiency.

In this study, LES is used for numerical investigation of vortex formations in a single dimple. From LES calculations a detailed insight is given for spatially resolved pressure distributions and instantaneous flow structures inside and around the dimple.

NUMERICAL METHOD

The LES equations are obtained by filtering the continuity equation, the Navier-Stokes equations and the transport equation for the temperature T at the filter width $\widetilde{\Delta}$:

$$\frac{\partial \widetilde{u_i}}{\partial x_i} = 0, \qquad (1)$$

$$\frac{\partial \widetilde{u}_i}{\partial t} + \frac{\partial \widetilde{u}_j \widetilde{u}_i}{\partial x_j} = -\frac{1}{\rho}\frac{\partial \widetilde{P}}{\partial x_i} + \frac{\partial}{\partial x_j}\left[\nu\left(\frac{\partial \widetilde{u}_i}{\partial x_j} + \frac{\partial \widetilde{u}_j}{\partial x_i}\right) - \tau_{ij}\right],$$
(2)

$$\frac{\partial \widetilde{T}}{\partial t} + \frac{\partial \widetilde{u}_j \widetilde{T}}{\partial x_j} = \frac{\partial}{\partial x_j}\left[\frac{\nu}{Pr}\frac{\partial \widetilde{T}}{\partial x_j} - J_j^{SGS}\right].$$
(3)

The unclosed subgrid stress tensor

$$\tau_{ij} = \widetilde{u_i u_j} - \widetilde{u}_i \widetilde{u}_j,$$
(4)

and the subgrid contribution to the scalar dynamics

$$J_j^{SGS} = \widetilde{T u_j} - \widetilde{T}\widetilde{u}_j$$
(5)

are modeled in terms of the filtered quantities $\widetilde{u}_i$ and $\widetilde{T}$. The unclosed stress tensor τ_{ij} is modeled using the dynamic mixed model (DMM) (Zang, 1993). To ensure the numerical stability of DMM calculations a clipping procedure derived from a rigorous mathematical analysis based on Taylor series approximation is applied (Kornev, 2007).
LES has been performed using the parallelized object oriented software OpenFOAM based on a 3-D finite volume method for arbitrary non orthogonal grids. The filtered transport equations are solved on a non staggered Cartesian grid, the discretisation in space and time of the transported and transporting quantities at the cell faces is of second order using central differencing scheme.
The molecular Prandtl number Pr was set to 0.7, whereas in LES the turbulent viscosity μ_t and the Prandtl number Pr_t are determined dynamically within the DMM. The Reynolds number based on the averaged bulk velocity U_b and dimple print diameter D was equal to $Re_D = 20000$ and $Re_D = 40000$.

COMPUTATIONAL GRID AND BOUNDARY CONDITIONS

The computational domain is shown in Figure 1 and was chosen to match conditions of experiments of Terekhov et. al. ($L_y = 15mm$, $L_z = 115mm$). The diameter D of the dimple with a sharp edge was kept constant at $D = 46mm$, whereas the dimple depth t was set to $t = 0.26D$. Periodic boundary conditions were applied in homogeneous spanwise direction. No slip boundary conditions were enforced on the lower and the upper channel walls. LES inlet conditions were specified using the precursor method and synthetic generation of turbulent fields by the method of Kornev et al. (2007) called inflowgenerator. For the precursor method a quasi periodic channel flow was calculated in front of the computational domain. The fluctuations and the mean velocity of the channel flow were used as inlet conditions of the computational domain. To drive the flow with a certain velocity U_b the overall losses within the channel were calculated and simply added as the driving force to the momentum equation. To reduce the amount of computational costs the inflowgenerator is also applied at the inlet. The integral length scales, needed for inflowgenerator, are taken from DNS by Moser et al. (1999). Since the inlet signal is correlated both in space and in time and the statistical properties are reproduced up to the second order, the transition area behind the inlet is relatively short.
In order to establish the grid independence of the LES model a series of calculations were carried out. On its base a block structured curvilinear grid consisting of 1'496'000 cells was chosen for further investigations. The number of cells inside the dimple was 9000, which is quite enough to resolve
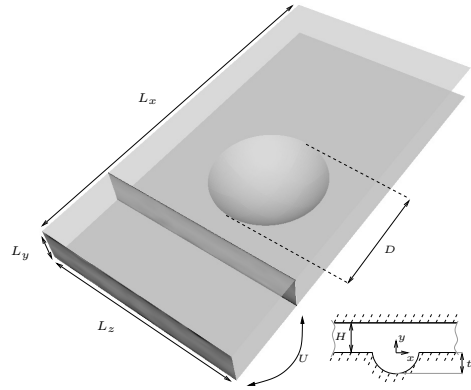
Figure 1: Computational domain of the channel with a single spherical dimple inserted at the lower wall.

the main vortex structures arising from the dimple surface. The stretching of grid cells was set to satisfy the condition $y^+ = 5$ for the fist grid point. The maximum values $y^+ = 5$ take place at some grid points at the downstream side of the dimple, whereas at all other locations y^+ is much less than five. Therefore, the first grid points were always located inside of the laminar sublayer.

RESULTS

The present numerical study is aimed to investigate vortex development in turbulent flow over a single dimple in a flat channel. The ratio of dimple depth to dimple print diameter is $t/D = 0.26$ whereas the ratio of channel height to dimple diameter H/D is 0.326. Numerical results include validation using experiments and DNS, vortex freqency analysis, flow visualisations and POD (proper orthogonal decomposition) analysis.

Validation

The inflow generation methods have been validated for the channel flow for a Reynolds number of $Re_\tau = 395$. Time and spatially averaged results, especially the shear stress $u'v'$ and transversal stress $w'w'$, show very good agreement to DNS data from Moser et al. (1999) for both inlet conditions.
Further numerical results are compared with experimental data published by Terekhov et al. (1997) for a smooth channel with a single dimple. Figure 2 shows the profile of normalized mean velocity obtained from LES and experiments along the y-axis at $x/H = 0.0$ and $z/H = 0.0$ at the center of the dimple. The data obtained for the Reynolds number of $Re_D = 40000$ are normalized by the maximum velocity U_0 determined in the center of the channel flow at $y = H/2, z = 0$ far upstream from the dimple. The dividing surface between the dimple and the channel passage is located at $y/H = 0$. Numerical results show good agreement with experimental data. Small discrepancy with measurements can be observed in the near wall region inside the cavity. The most probable reason for the discrepancy between theory and experiment in this region might be typical LDA measurements problems in close proximity to the wall. The strongest velocity gradients are detected at the channel walls and on the dividing surface. Furthermore, the dividing surface separates areas of positive and negative time averaged axial velocities. With the other words, the dividing surface $y/H = 0$ is the time averaged border of

Sixth International Symposium on Turbulence and Shear Flow Phenomena
Seoul, Korea, 22-24 June 2009

the recirculation area arising inside the dimple. Strong vortices generated on the border of the recirculation zone at $y/H \sim 0$, due to instability of the shear layer development, produce significant pulsations. The fluctuations across the channel height is shown in figure 3. A discrepancy between numerics and measurements is observed in location of the maxiumum of the u-rms value. LES predict the largest fluctuations exactly on the dividing surface whereas the measured maximum of u-rms lies inside the dimple. However, it should be noted that the numerical results seem to be reasonable. Indeed, the maximum pulsations occur in the area of the strongest velocity gradients which is in accordance with well tried turbulence closure models.
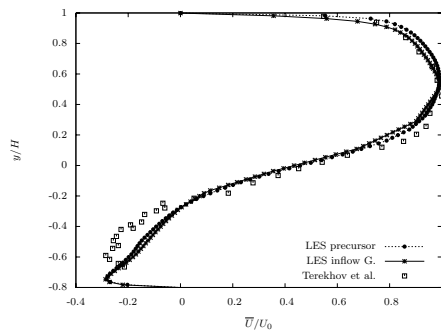
Figure 2: Mean velocity profile across the channel height at $x/H = 0.0$ obtained from LES with different inlet conditions in comparison with experiments of Terekhov et al. (1997).
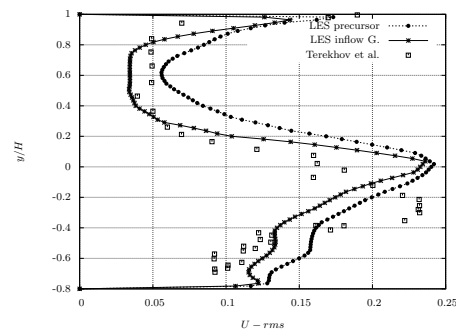
Figure 3: Distribution of the normal stress in axial direction across the channel height in the center of cavity $x/H = 0.0$ in comparison with measurements of Terekhov et al..

Finally the distribution of the dimensionless pressure coefficient C_p

$$C_p = \frac{(P - P_0)}{\rho U_b^2 / 2} \qquad (6)$$

along the centerline in streamwise direction in flow direction at the dimpled wall is shown in figure 4. P_0 is the pressure calculated at position $x/D = -1$. In front of the dimple edge at the downstream side of the cavity the pressure coefficient experiences a high increase. This effect is caused by a stagnation of the main channel flow which collides with the windward dimple side. A dramatic pressure loss happens further downstream where the flow is passed over the rear sharp edge of the dimple.

The results presented in Fig. 2, 3, 4 show that LES is ca-
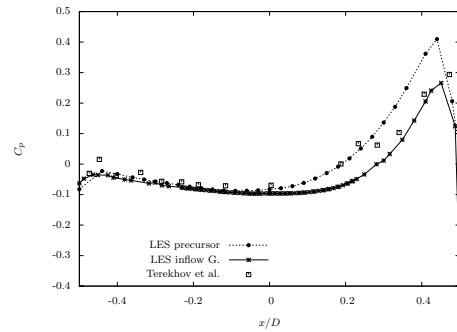
Figure 4: Distribution of the pressure coefficient C_p along the centerline in streamwise direction at the dimpled wall for $Re_D = 40000$.

pable of predicting the flow in a dimpled channel with a satisfactory accuracy.

Flow Structure

The distributions of mean velocities presented in figure 2 shows clearly the creation of a large recirculation zone within the dimple. The time averaged profile occupies about 90% of the cavity. The core of the reverse flow is located slightly downstream with respect to the cavity center. The most interesting physical phenomenon of the dimple flow is the presence of auto oscillations described in experiments by Kiknadze et al. (1990), Terekhov et al. (1997) and Won et al. (2005).

Self-sustained oscillations in dimple. The appearance of organized self-sustained oscillations is a typical phenomenon for flows with a massive separation. In spite of many similarities there are significant differences in formation of structures responsible for such oscillations depending on the geometry and Reynolds number. Terekhov et al. (1997) observed visually transversal oscillations of the flow inside the dimple with the depth to diameter ratio of $t/D = 0.26$ using hydrogene bubbles. These oscillations have low-frequency and high-frequency components. The low frequency oscillations occur as aperiodical outbursts with an angle of $\alpha = 45°$ with respect to the mean flow direction. Streamlines from early URANS (Isaev, 2003) simulations indicate the presence of an asymmetric vortex structure inclined to the mean flow direction at the angle of approximately $\alpha = 45°$. In contrast to experimental observations the asymmetric structure gained from URANS is steady and can be detected in time averaged flow pattern. LES results also reveal the formation of asymmetric structures but in contrast they are unsteady. Since instantaneous flow snapshots from LES look very chaotically the analysis is performed for characteristics averaged locally in time. Figure 5 shows streamlines averaged within three sec of real time at differtent time instants. Streamlines indicate the asymmetrical vortex structures inclined to the mean flow. The coherent vortex structure is switched nearly periodically from the position $\alpha = +45°$ to the position $\alpha = -45°$. Therefore, for a hole with a depth to diameter ratio of $t/D = 0.26$, numerical results confirm the generation of unsteady asymmetric monocore vortex structures with a predominant transversal direction. As seen from instantaneous streamlines patterns, the fluid flows directly from the channel into the dimple and rotates within the recirculation zone and finally flows out at the dimple end. The presence of the vortices is also clearly confirmed in the
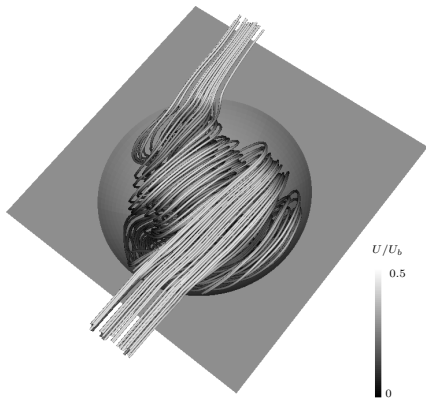
(a)
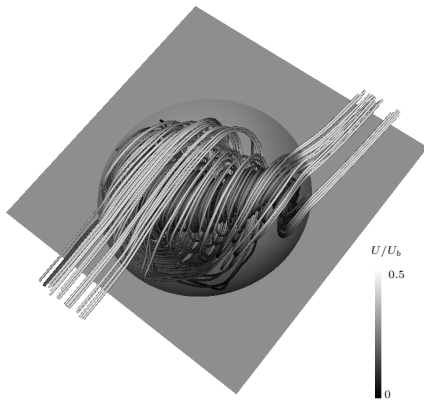
(b)

Figure 5: Vortex structures obtained from LES velocity field averaged over averaged three sec realtime for different flow periods . $Re_D = 40000$.

pictures of the pressure iso surfaces showing low pressure areas inside of the dimple inclined to the mean flow. However, the flow averaged over a sufficiently long time period is nearly symmetric. In this context LES results and qualitative measurement observations contradict to URANS ones which predict the asymmetry even in the averaged flow pictures. The switching is also reflected in the time history of longitudinal velocity u_x recorded at two symmetric points at $x/H = 0, y/H = 0, z/H = \pm 0.66$ (figure 6). Two following conclusions can be drawn from the diagram analysis. First, the presence of long period self-sustained oscillations is obvious. Second, there is a sort of opposition-of-phase of the flow. Once the flow is accelerated at the point $z/H = -0.66$ it is decelerated or even changes the direction at the point $z/H = 0.66$. This effect can be explained by consideration of the mutual position of the vortex structure and the selected points. The vortex is inclined both in horizontal and vertical directions. The vortex inlet is located deeply inside of the dimple whereas the outlet is above the dimple edge downstream. Such a vortex induces both positive and negative longitudinal velocities depending on the point location. At the position $\alpha = +45^o$ (figure 5a) the point $z/H = +0.66$ lies above the vortex core which induces the positive velocity resulting in the flow acceleration. The point $z/H = -0.66$ can be located either under the vortex axis, above or close to it. In the first case we have negative induced velocity, in
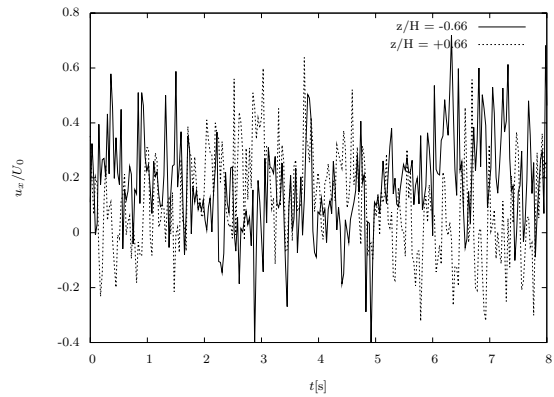
Figure 6: Time history of longitudinal velocity u_x recorded at two symmetric points at
$x/H = 0, y/H = 0, z/H = \pm 0.66$ at $Re_D = 40000$.

the second case the induced velocity is lowered. The situation is changed when the vortex position is switched. The flow acceleration takes place at $z/H = -0.66$ whereas the flow at $z/H = 0.66$ is decelerated. In both cases the product of pulsations at both points is negative. As a result the autocorrelation function

$$R_{uu}(\eta) = \overline{u'_x(x,y,z)u'_x(x,y,z+\eta)}/\overline{u'_x(x,y,z)^2}$$

calculated at these two points changes its sign in transversal direction (figure 7).
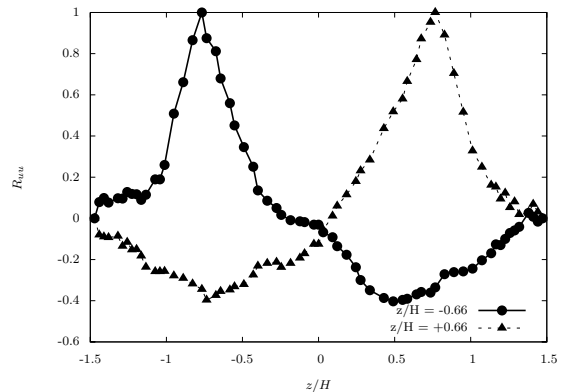
Figure 7: Samples of two point correlations R_{uu} across the dimple crosssection z/D at $x/D = 0.0$ $Re_D = 40000$.

In experiments of Terekhov et al. (1997) oscillations with frequencies varying from $0.05Hz$ to $0.2Hz$ were detected. To prove this fact the time history of the longitudinal velocity containing about 50000 time steps was recorded from LES and statistically evaluated at two spatial points with coordinates $x/H = 1.0, z/H = +0.66$ (point 1) and $x/H = 1.0, z/H = -0.66$ (point 2). Figure 8 presents the normalized frequency spectrum. A clear peak in the frequency spectrum around $f = 0.48Hz$ for the point 1 and $f = 0.23Hz$ for the point 2 can be observed at $Re_D = 40000$. For the case $Re_D = 20000$ a peak at $f = 0.23Hz$ is documented at both points. Analysis of streamline patterns and frequencies indicates the presence of periodic outbursts near the back side of the dimple. The second dominating frequency of about $10Hz$ is observed only at the point 1 for $Re_D = 40000$. This fact underlines again the unsteady flow asymmetry although the averaged flow seems to be symmetric.

Sixth International Symposium on Turbulence and Shear Flow Phenomena
Seoul, Korea, 22-24 June 2009
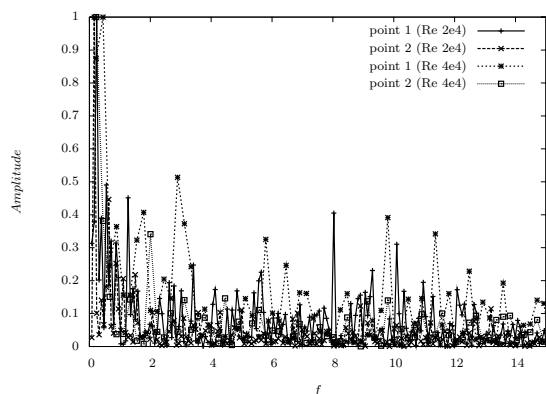
Figure 8: Normalized frequency spectrum at point 1 and point 2 for $Re_D = 40000$.

POD Analysis.

The main goal of the POD procedure is the structure recognition in a certain unsteady field of different quantities. POD technique originally proposed by Lumley (1970) for turbulent flows is based on the Karhunen-Leòve decomposition. This technique is very usefull for identification of spatial structures and estimation of their contributions to the total energy of the flow field. The field is represented in the form of series of products of space dependent functions $\Phi_i^{(n)}(\mathbf{x})$ and time dependent coefficients $a^{(n)}(t)$.

$$u_i(\mathbf{x}, t) = \sum_{n=1}^{N} a^{(n)}(t)\Phi_i^{(n)}(\mathbf{x}) \qquad (7)$$

The turbulent field $u_i(\mathbf{x}, t)$ is taken from numerical simulations. For application of POD the snapshot method proposed by Sirovich (1995) is used for decomposition of high dimensional fields like the velocity field $\mathbf{u}(\mathbf{x}, t)$. The POD procedure is especially efficient if a restricted number of first modes contain the most of the overall energy. The POD results presented below have been obtained using 1100 samples of the velocity and pressure fields. At the time step of $\Delta t = 0.01$ this sampling corresponds to 11 sec of real time. The energy contribution of different modes decreases rapidly within the first 25 modes. The first 40 modes represent about 25% of the energy at $Re_D = 4 \cdot 10^4$ whereas 51 modes at $Re_D = 2 \cdot 10^4$. The presence of dominating modes is most pronounced for $Re_D = 4 \cdot 10^4$. In this case the modes $n = 1$ and $n = 2$ play a dominant role in the energy budget. Also at $Re_D = 2 \cdot 10^4$ the first two modes are dominant. However, the superiority of their contributions is less in comparison with case of $Re_D = 4 \cdot 10^4$. It is in accordance with the concept that the turbulent fields show tendency to formation of strong concentrated structures unevenly distributed in space when the Reynolds number increases.
Since the streamlines for $Re_D = 2 \cdot 10^4$ look similarly to $Re_D = 4 \cdot 10^4$ they are not presented. Figure 9 shows the streamlines of first and second spatial functions $\Phi^{(1)}$ and $\Phi^{(2)}$ for $Re_D = 4 \cdot 10^4$. The structure corresponding to the first eigenflow arising close to the end of the dimple looks like a "tornado" taking its origin inside the dimple and penetrating into the channel. This structure can be interpreted as the tornado-like structure or the so called mono cell structure analogously to the structure described by Isaev (2003). The structure is centered at the midpoint of the cavity and rotates around the y-axis. It transports the fluid from the dimple into the channel at an angle of approximately $\alpha = 45$

(a)

(b)
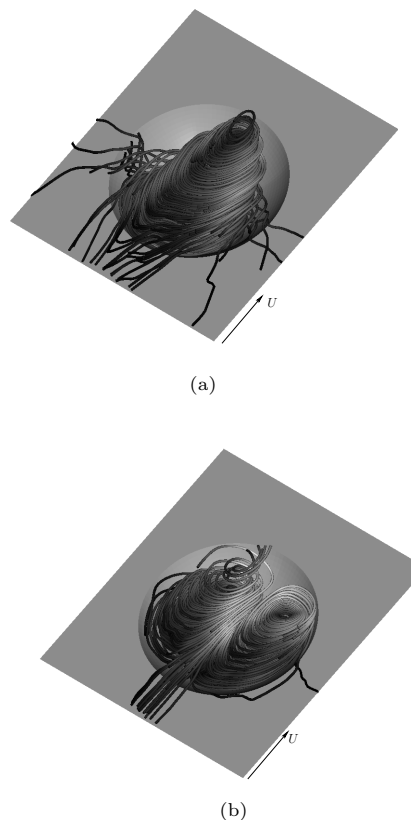
Figure 9: Streamlines of the first $\Phi^{(1)}$ (a) and second $\Phi^{(2)}$ (b) spatial modes obtained from POD of the velocity field at $Re_D = 4 \cdot 10^4$.

deg measured from the main flow direction. The streamlines coming into the dimple from adjacent plate surface indicate clearly that the structure has a significant impact not only on the flow inside the dimple but also on the flow on the plate around the dimple. Obviously it causes an increased heat transport. Also two structures corresponding to the second mode are tornado like spatial structures. In contrast to the second mode structure they are symmetric about the centerline. From the temporal coefficients $a^{(1)}(t)$ normalized by its maximal value $a_{max}^{(2)}$ versus time for the first POD mode, a drastic alternation from negative to positive values can be observed for both Reynolds numbers. Physically, the sign change of $a^{(1)}(t)$ means that the first mode structure steadily changes their rotation direction. To a certain extent, the results are consistent with results obtained from the direct analysis of structures presented in the previous subsection. Periodical change of the rotation direction of the second mode is an additional explanation of long period oscillations with the opposition-of-phase mentioned above. This leads to periodic transversal fluctuations and outbursts at the back side of the cavity observed in measurements. However, it should be noted that such structure is not seen in the flow pattern pictures. The so called tornado like structures widely mentioned in the literature seem to be a fiction rather than a really existing coherent structures. The second mode structures reflect a collective action of vortices of different size and orientations producing the self-sustained oscillations conducted with the opposition-of-phase motion. The iso-surfaces of POD structures of the pressure field are shown in figure 10. For both Reynolds numbers the first spatial mode structure of the pressure field indicate the vortices

arising in the shear flow separating the main flow and the recirculation zone in the dimple. The iso-surfaces are almost symmetric with respect to the longitudinal symmetry plane of the flow.
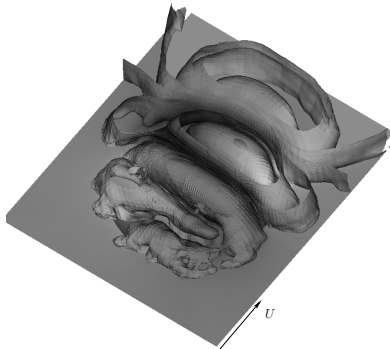
Figure 10: Iso-surfaces of the first spatial mode obtained from POD of pressure field at $Re_D = 4 \cdot 10^4$.

Conclusion

Comparison of numerical results with experiments of Terekhov et al. (1997) shows that LES models are capable of predicting the averaged flow in a symmetry plane of a dimpled channel with a satisfactory accuracy.

LES reveal the presence of oscillations with dominating frequencies inside the flow over a single dimple. The same conclusion has been drawn in many measurements on dimples. At selected points inside of the dimple these oscillations have low-frequency and high-frequency components whereas at other points only a dominating low-frequency component can be distinguished. Analysis of flow structures using instantaneous streamlines and pressure iso-surfaces shows clearly the presence of the coherent vortex structure which is inclined with respect to the incoming flow. The vortex orientation is changed nearly periodically in time causing long-period oscillations with the opposition-of-phase motion. Although the instantaneous flow is asymmetric, however, the flow averaged over a sufficiently long time period is nearly symmetric. In this context LES results contradicts to early URANS simulations which predict the asymmetry even in the averaged flow pictures. Since the experimental averaged field is also symmetric, LES reproduces the flow physics more correctly than URANS. POD analysis revealed formation of tornado like spatial structures inside the dimple. The first POD mode corresponds to a mono structure steadily changing its rotation in time. Most probably this structure is responsible for periodic fluctuations and outbursts at the back side of the cavity. The second mode corresponds to a twin structure located symmetrically inside the dimple.

REFERENCES

Chyu M.K., Yu Y., Ding H., Downs J.P., Soechting F., 1997, "Concavity enhanced heat transfer in an internal cooling passage", *ASME Paper* No 97-GT-437.

Gromov P.R., Zobnin A., Rabinovich M.I., and Sushik M.M., 1986, "Creation of solitary vortices in a flow around shallow spherical depressions", *Sov. Tech. Phys. Lett*, No.12, 547.

Terekhov V.I., Kalinina S.V., Mshvidobadse Y.M., 1997, "Heat transfer coefficient and aerodynamic resistance on a

surface with a single dimple", *Enhanced Heat Transfer* Vol. 4, pp. 131145.

Mahmood G.I., Hill M.L., Nelson D.L., Ligrani P.M., 2000, "Local heat transfer and flow structure on and above a dimpled surface in a channel", *ASME Paper* No. 2000-GT-230

Won S.Y., Zhang Q., Ligrani P.M., 2005, "Comparisons of flow structure above dimpled surface with different dimple depths in a channel", *Physics of Fluids* Vol. 17 No. 045105

Ligrani P.M., Harrison J.L., Mahmood G.I., Hill M.L., 2001, "Flow structure due to dimple depressions on a channel surface", *Physics of Fluids*, Vol.13., N11., pp. 3442-3448.

Isaev SA, Leont'ev, A.I., 2003, "Vortex enhancement of heat transfer under conditions of turbulent flow past a spherical dimple on the wall of a narrow channel", *High Temperature*, Vol. 41., No. 5, pp 655-679.

Zang Y.,Street R.L., Koseff J.R., 1993, A dynamic mixed subgrid-scale model and its application to turbulent recirculating flow, *Physics of Fluids*, A5:12:31863196.

Kornev N.V. ,Tkatchenko I., Hassel E., 2006, A simple clipping procedure for the dynamic mixed model based on Taylor series approximation, *Commun. Numer. Meth. Engng.*, Vol. 22, pp. 55-61.

N. Kornev, H. Kroeger, E. Hassel, 2007, "Synthesis of homogeneous anisotropic turbulent fields with prescribed second-order statistics by the random spots method", *Commun. Numer. Meth. Engng.*, Vol. 24, pp. 875-877.

R.D. Moser, J. Kim, N.N. Mansour, 1999, "Direct numerical simulation of turbulent channel flow up to $Re_\tau = 590$", *Physics of Fluids*, Vol.11., pp. 943-948. . M.m, Kawamura T.,Mabuchi J., Kumada M., 1983, "Some characteristics of flow pattern and heat transfer past a circular cylindrical cavity", *JSME* Vol. 26 (220), pp. 1744

Kiknadze G.I., Oleinikov V.G., 1990, "Self-organization of tornado-like vortex structures in gas and liquid flows and heat transfer intensification", *Proc. Inst. Thermophysics Preprint 227*, Novosibirsk,p. 46

Lumley J., 1970, "Stochastic Tools in turbulence", *Academic Press*, New York

Berkooz G., Holmes P., Lumley J.L., 1993, "The proper orthogonal decomposition in the analysis of turbulent flows", *Ann. Rev. Fluid Mech.* Vol. 25, pp. 539576

Sirovich L., 1987, "Turbulence and the Dynamic of Coherent Structures Part 1-3", *Quarterly of Applied Mathematics*, 45 No. 3, pp. 561-590

Isaev S.A., Leontev A.I., Mitjakov A.V., Pyshnyi I.A., 2003, "Intensification of tornado-like heat transfer in asymmetric dimples", *J. Engineering Physics and Thermophysics*, Vol. 76, pp. 3134